Study on a Supercritical Airfoil Using Tilted Microjet

Abhishek Rawat
Amity Institute of Aerospace Engineering, Amity University Uttar Pradesh, Noida, Uttar Pradesh, 201313, India

***Abstract*—Gust loads represent a critical design constraint for civil transport aircraft, directly influencing structural weight, fatigue life, and passenger comfort. Conventional gust load alleviation strategies rely on moving-surface control devices such as flaps and ailerons; however, their large inertia limits effective response to low-frequency disturbances, leaving higher-frequency gust loads to be absorbed structurally. Recent advances in active flow control have introduced mechanical and fluidic microactuators as promising alternatives for high-frequency load mitigation. In this study, the effectiveness of fluidic microjets for aerodynamic load control is investigated numerically at subsonic and transonic conditions. Simulations are performed on the RAE 2822 airfoil equipped with a trailing-edge microjet using the Reynolds-averaged Navier–Stokes equations solved with the CFL3D solver. Both conventional normal jets and upstream-directed microjets are examined at a fixed momentum coefficient. The results demonstrate that fluidic actuation provides a nearly linear lift reduction with respect to the square root of the momentum coefficient. While both jet configurations effectively reduce lift, upstream-directed jets achieve superior load alleviation by enlarging the separation region and increasing suction-side pressure. Furthermore, at transonic speeds, upstream jets mitigate shock-induced drag penalties, resulting in lower overall power consumption compared to normal jets. These findings highlight the potential of upstream fluidic microjets as an efficient and reliable solution for gust load alleviation in future transport aircraft.**

***Index Terms*—Gust load alleviation; Active flow control; Fluidic microjets; Aerodynamic load control; Upstream jet blowing**

I. INTRODUCTION

A significant influence on civil transport aircraft designs comes from gust loads [1]. An aircraft's structural weight can be lowered as a result of mitigating the effects of gust loads [2]. Additionally enhancing passenger comfort will make it much more competitive. Traditionally, to optimize load distribution during gust encounters and maneuvers, moving surface control systems [3, 4] have been used. These systems frequently make use of the current control surfaces, including spoilers, flaps, and ailerons. These actuators, however, have a rather large moment of inertia because they were originally intended for aircraft maneuvers.

Typically, ailerons and flaps have an effective reaction frequency of less than 10 Hz, hence higher frequency gust loads must be carried at the expense of additional construction weight by the aircraft structure. Modern technology has led to the development of mechanical or fluidic microactuators, which are able to reduce gust loads that are too strong for conventional devices. The application of micro actuators to flow control has long been studied.

The reliability of the system is decreased when spanwise-distributed microtabs are deployed because it takes numerous mechanical structures to cooperate, even though the mechanical microtabs may produce a high frequency response. Furthermore, the lift modification generated The design of the control system is made more difficult since the amount by the microtab is not exactly $proportionate\ to\ the\ tab\ height$ [5].

In contrast, fluid actuators are relatively simple, requiring only a small number of valves for control. Moreover, the lift reduction produced by the fluid actuators was observed to be approximately linear with respect to the square root of the momentum coefficient, defined as:

$$\dot{m}U_j l\left(\frac{1}{2}\right)\rho_\infty \cup_\infty^2 c$$

where m_ is the jet mass flow rate, Uj is the jet velocity magnitude, $\left(\frac{1}{2}\right)\rho_\infty \cup_\infty^2 c$ is the freestream dynamic pressure, and c is the chord length.

II. LITERATURE REVIEW

In recent years, Modern technology has led to the development of mechanical or fluidic microactuators, which are able to reduce gust loads that are too strong for conventional devices. The application of microactuators to flow control has long been studied. As an example, They were applied to raise lift [7, 8], avoid separations [6], and postpone transitions [9].
Khalil et al. [10] numerically compared the efficiency of various load control actuators.

They discovered that fluidic actuators' lift and pitching moment responses were comparable. Compared to traditional flaps, these fluid actuators often had a lower drag penalty than mechanical ones. Notably, Coanda jets require a smaller momentum coefficient for the same lift decrease as regular jets. But using Coanda jets often yields a thick, rounded trailing edge, which, while in cruise, will increase drag on the aircraft [11]. Furthermore, Coanda jet holes are often smaller than regular jet holes, which means that at transonic speeds, they have a poorer efficiency and greater jet velocities [12, 11].

AlBattal et al. [13, 14] promoted and experimentally examined surface blowing as a means of active aerodynamic load reduction at low speeds. They concluded that the jet perpendicular to the airfoil surface was wasteful and suggested using the upstream jet in place of the traditional normal jet..

During the experiment, a thin deflection piece blocks the normal expelled air and forces it to be redirected 90 degrees in the direction of the upstream flow. The rear stagnation point is moved forward by the upstream blowing, creating a bigger recirculation zone and altering the effective camber

III. METHODS

AIRFOIL GEOMETRY:
An investigation was completed to determine the level of detail needed in the modeling of the microjet.
RAE 2822 is used as a geometry. Chord length taken 100 mm.
Microject is placed at 95% of chord length in upper surface of airfoil .
Slit weidth " h_j" is 0.2 -1% of x/c .

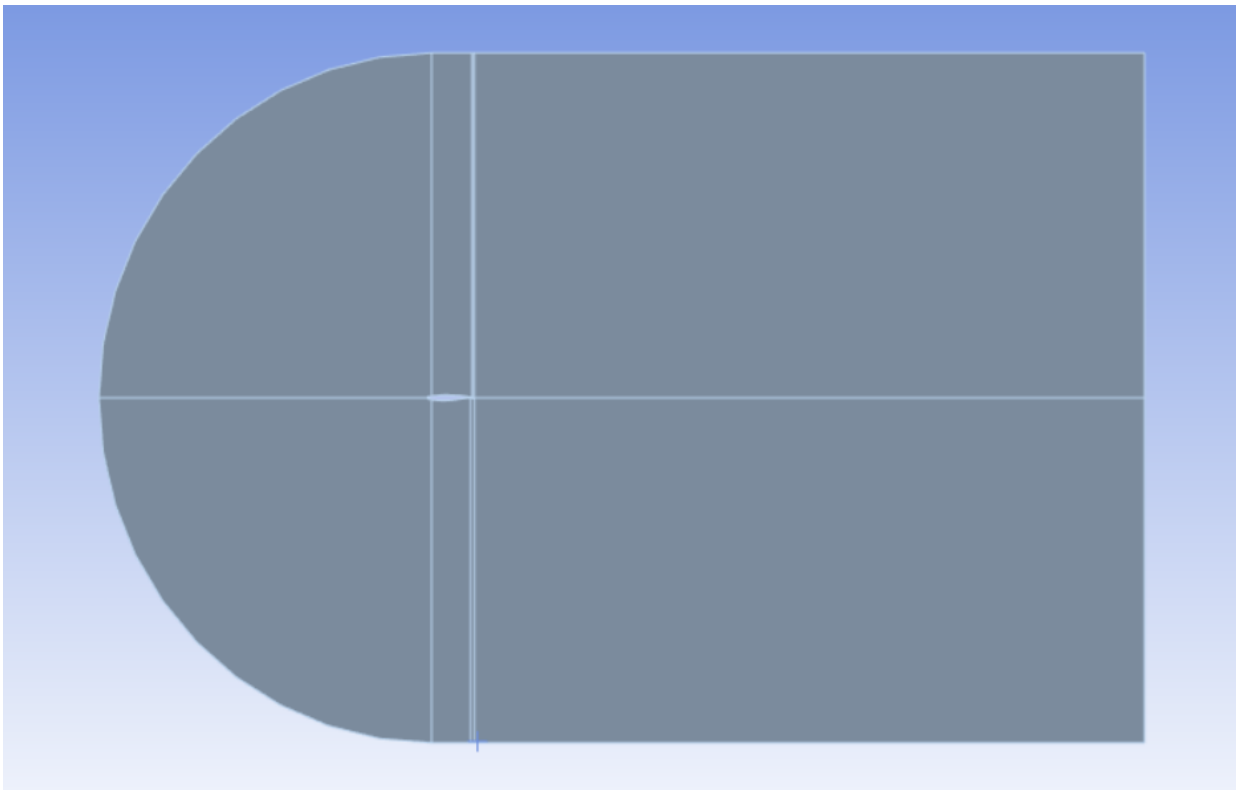

Figure 1 geometry of rae 2822

IV. MESH GENERATION

The far-field boundary is extruded 15c away from the airfoil surface. Figure 2 shows the generated grid around the RAE 2822 airfoil equipped with a normal microjet . The grid contains a total
33109 nodes and 32725 elements.

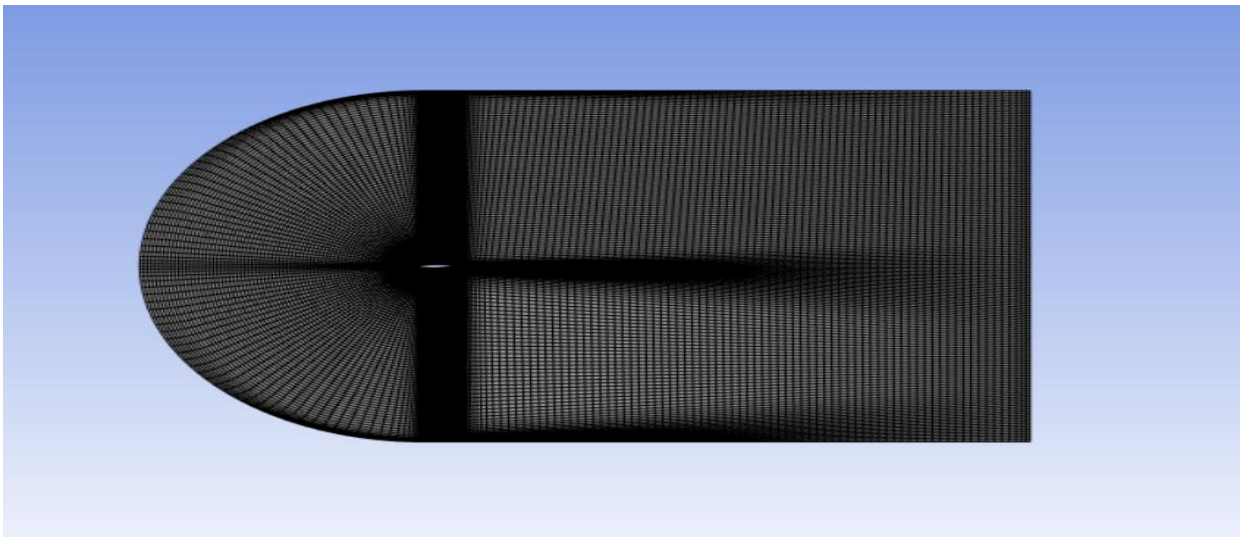

Figure 2 mesh

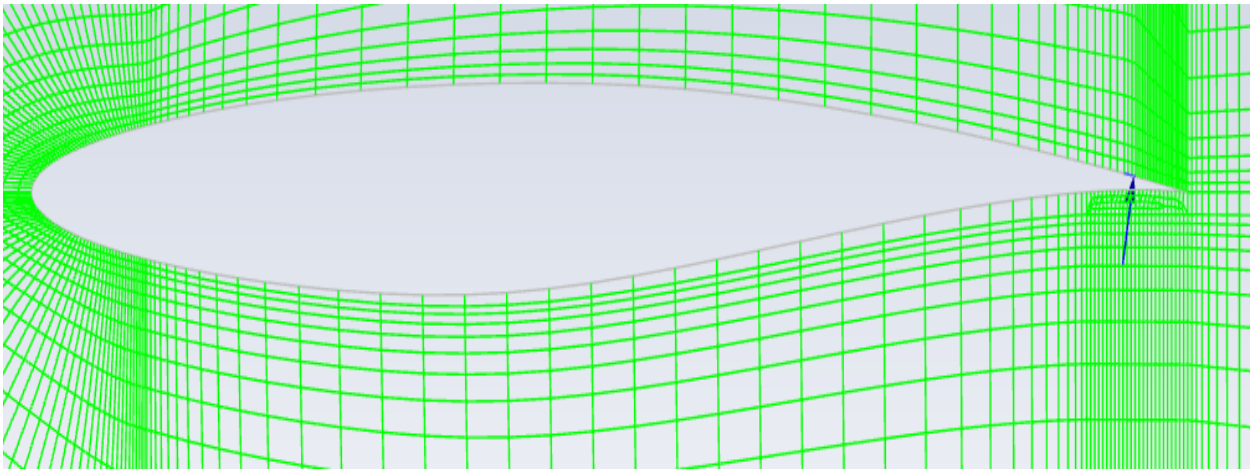

Figure 3 Mesh topology

V. MOMENTUM COEFFICIENT

The jet intensity is usually described using the momentum coefficient

$$C_\mu = \frac{\rho_J \bigcup_J^2 h_J}{\frac{1}{2}\rho_\infty \bigcup_\infty^2 C}$$

where ρj is the injection density, Uj is the injection velocity, hj is the slit width, $\frac{1}{2}\rho_\infty \bigcup_\infty^2 C$ is the freestream dynamic pressure, and c is the chord length. In this study, the momentum coefficient is set to Cμ = 0:005 so that the jet velocity magnitude Uj equals the freestream velocity U∞ in an incompressible flow.

VI. POWER CONSUMPTION

The jet injection can be achieved by compressing the air with a compressor. According to the analysis by

Lefebvre et al. [18], the power consumption can be determined as the following:

$$p_{Jet} = \frac{\dot{m}CpT_{01}}{\eta}\Gamma(\gamma-1)/\gamma - 1$$

where m_ is the mass flow rate, T01 is the total temperature of jet flow, and Γ = p01/p00 is the total pressure ratio of the pump. p01 is the mass-weighted averaged total pressure of the jet flow. In this study, it is assumed that the pump inlet conditions are the same as freestream total conditions, and the compression is adiabatic. Thus, T01 is taken to be the freestream total temperature T0∞ and p00 is taken to be the freestream total pressure p0∞. η is the pump efficiency, which is taken to be 1.0 in this study to express the power required to drive the jet. The power consumption can be nondimensionalized with the free-stream dynamic pressure ð1/2Þρ∞U2 ∞, free-stream velocity magnitude U∞, and chord length c:

$$C_{Power} = P_{jet}/(\tfrac{1}{2})\rho_{\infty}U_{\infty}^{3}c$$

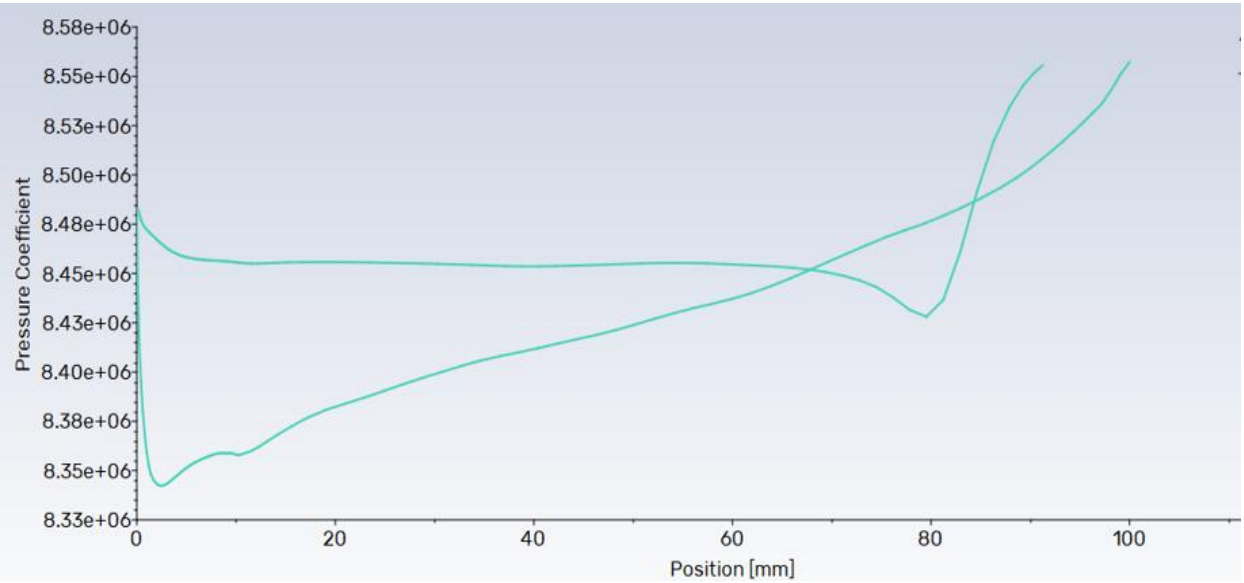

Figure 4 Pressure coefficient of airfoil RAE2822 at α =0°

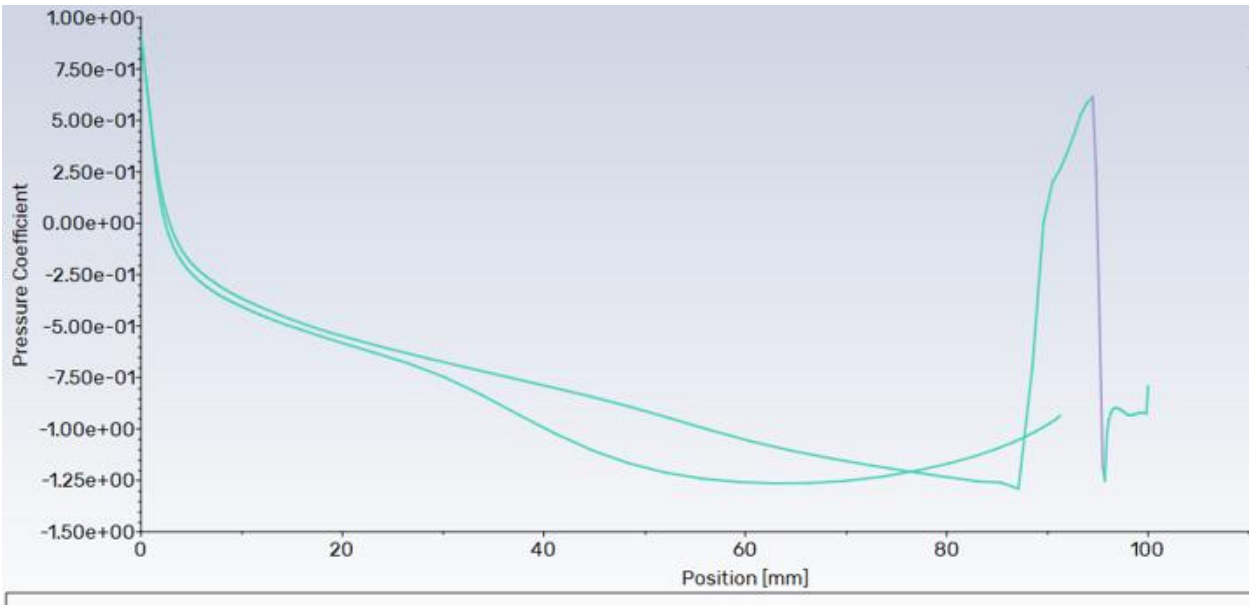

Figure 5 Pressure coefficient of airfoil RAE2822 with microjet at α =0°

VII. NUMERICAL METHODS

The open-source CFL3D code has been used to model the flows around the airfoil using microjets [15]. A solution to the compressible Navier-Stokes equations with Reynolds averages on multiblock structured grids The vector form of the two-dimensional compressible Navier-Stokes equation is

$$\frac{\partial Q}{\partial t}+\frac{\partial(f-fv)}{\partial x}+\frac{\partial(G-Gv)}{\partial y}=0$$

Where $Q=\left[\rho,\rho_{u,},\rho v,E\right]^{T}$ is the vector of conserved variables, consisting of the density, momentum, and total energy per unit volume. F and G are the convective flux terms. Fv and Gv are the viscous flux terms. The third-order upwindbiased MUSCL [16] scheme is chosen for the convective terms, and the second-order central differencing scheme is chosen for the viscous terms.

Blaylock et al. [17] compared three jet models—a resolved plenum, a uniform velocity inlet, and a velocity inlet with a parabolic profile—in order to replicate the jet flow. Their analysis demonstrates how little these models differ from one another. For incompressible materials, the velocity inlet technique with specified density and velocity is sufficient.

flows. Nonetheless, for transonic flows, it is challenging to calculate the jet flow density. Lefebvre et al. [18] fixed the injection cavity's overall temperature and adjusted its overall pressure to reach the desired Cμ.

VIII. FORCE CALCULATION

The lift, drag, and pitching moment are automatically integrated along the wall and jet boundaries during the solving process. However, the reaction force caused by the change in jet momentum also needs to be included. This reaction force r can be calculated by

$$\vec{r}=-\dot{m}\left(\overrightarrow{u_j}-\overrightarrow{u_\infty}\right)$$

where m is the jet mass flow rate, $u_j$is the jet velocity vector, and u_∞ is the freestream velocity vector. The reaction force applied at the jet center is incorporated into the overall lift, drag, and pitching moment., the aerodynamic coefficients of the airfoil can be calculated and corrected by the following equations:

$$c_L=\frac{L+Lv}{(1/2)\rho_\infty \cup_\infty^2 C}$$

$$C_d=\frac{Da+Dr}{\left(\frac{1}{2}\right)\rho_\infty \cup_\infty^2 C}+max(0,C_{Power})$$

$$C_m=\frac{Ma+Mr}{\left(\frac{1}{2}\right)\rho_\infty \cup_\infty^2 C}$$

where L, D, and M are the lift, drag, and pitching moment, respectively. Subscript ‘a’ indicates the value obtained with surface integration, while subscript ‘r’ indicates the contribution of the reaction force.

IX. VALIDATION FOR NORMAL MICROJET

Eggert et al. [19] evaluated RANS using CFL3D code to predict the effects of
active flow control by blowing from the leading-edge slot on the NACA 0018 airfoil.
CFL3D code utilizing RANS predicted identical flow characteristics to those seen in the experimental data, with a freestream Mach number of 0.03265. By using the computational and experimental results from the work of de Vries et al. [20], the existing approach for normal microjet is validated.
The studies were conducted based on the NACA0018 airfoil with microjet placing at x/c= 0.9 .
On the NACA0018 airfoil lower surface, the experimental model employed by de Vries et al. [20] has c= 0.165 m and jet width hjet= 0.001 m positioned at x/c= 0.9. The freestream characteristics are Rec = 6.6×105 and M∞ = 0.176. There is 1.2U∞ of blowing velocity. On the surface of the airfoil, the pressure was only recorded at four locations. A numerical research was also carried out by de Vries et al. [20] using the commercial computational fluid dynamics software program ANSYS CFX 11.0. When the incoming flow condition was the same as during the experiment, the total lift differences between the airfoils with and without microjet were assessed.
Figure below gives the comparisons of the calculated pressure distributions on models with and without microjet to the experimental data from Ref. [20]. The comparison shows a good agreement, especially for pressures on the upper surface. Fig. presents the comparisons of the changes of lift coefficients between the present results and the reference data. In general,

these results show a good match for both the models with and without microjet. It is also clear that the lift coefficient augmentation ΔCL≈ 0.4 is obtained due to the microjet with Ujet= 1.2U∞.

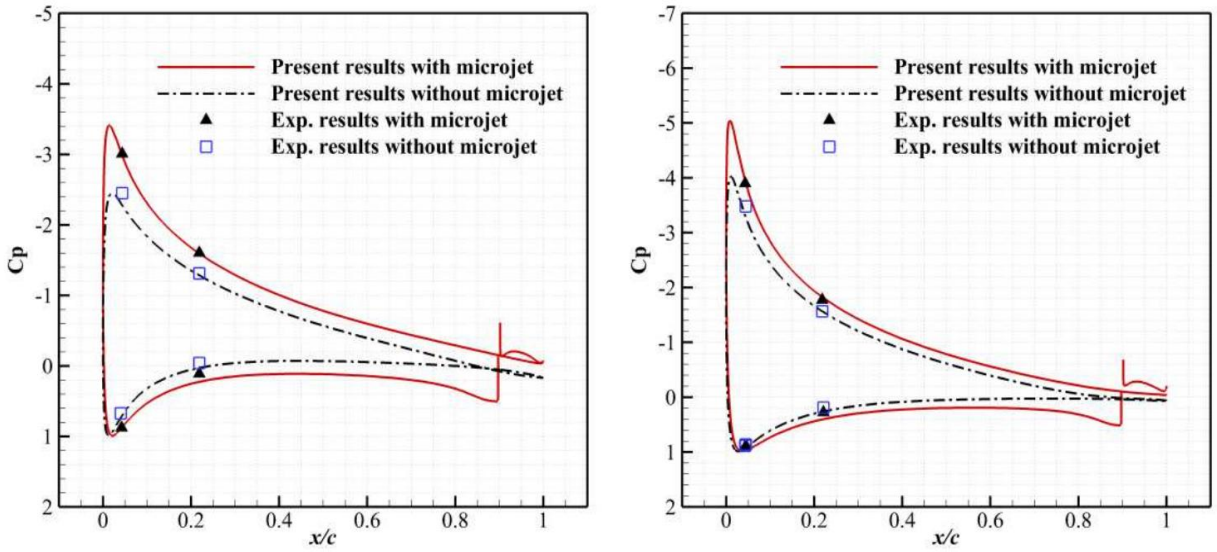

(a) α=8º (b) α=12º

Figure 6 pressure distribution

X. RESULT

Grid Sensitivity Study. A grid sensitivity study based on the RAE2822 airfoil was carried out to ensure that the overall forces are no longer sensitive to the computational grid.

Cl and Cm obtained for aerofoil rae 2822 without microject at α =0 at mach M=0.8

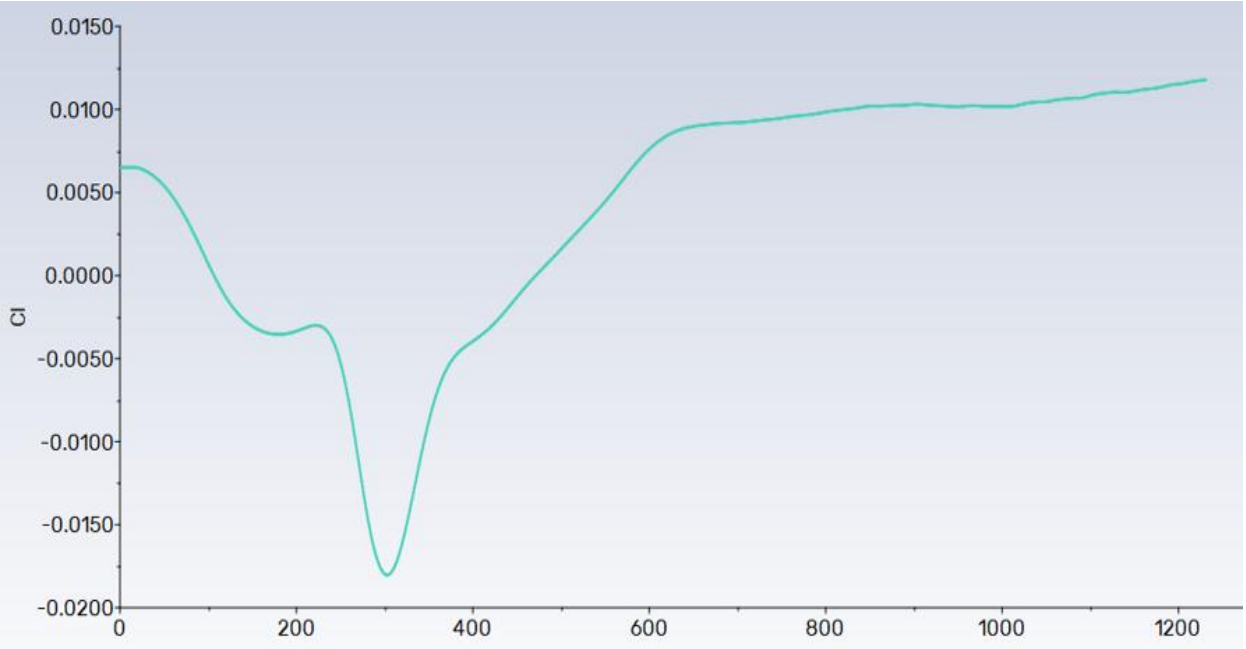

Figure 7 Cl without microjet at α =0

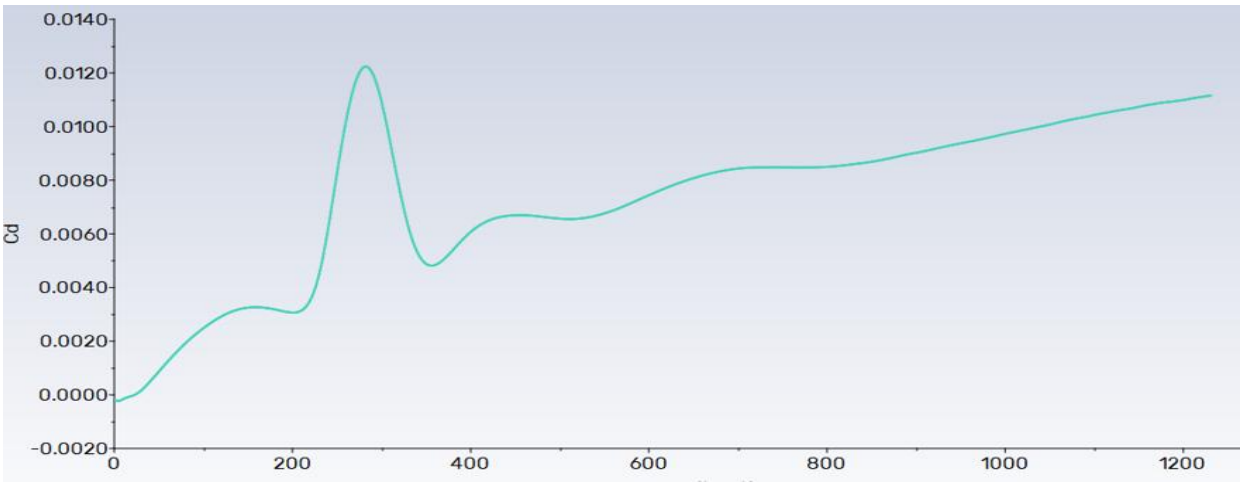

Figure 8 Cd without microjet at α =0

Cl and Cd obtained for aerofoil rae 2822 with microject at α =0° at mach M=0.8

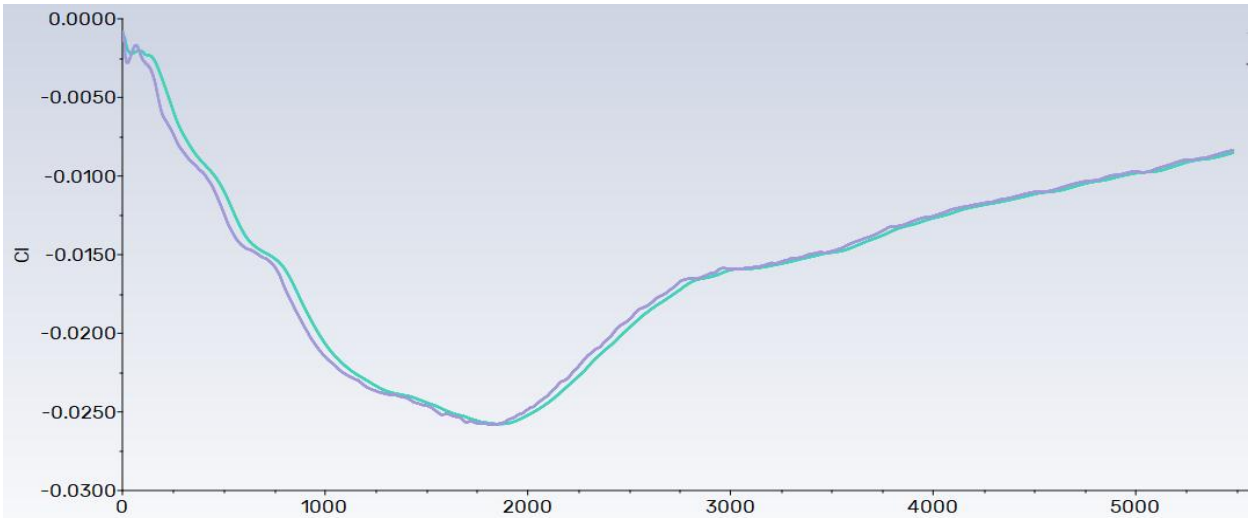

Figure 9 Cl with microjet at α =0

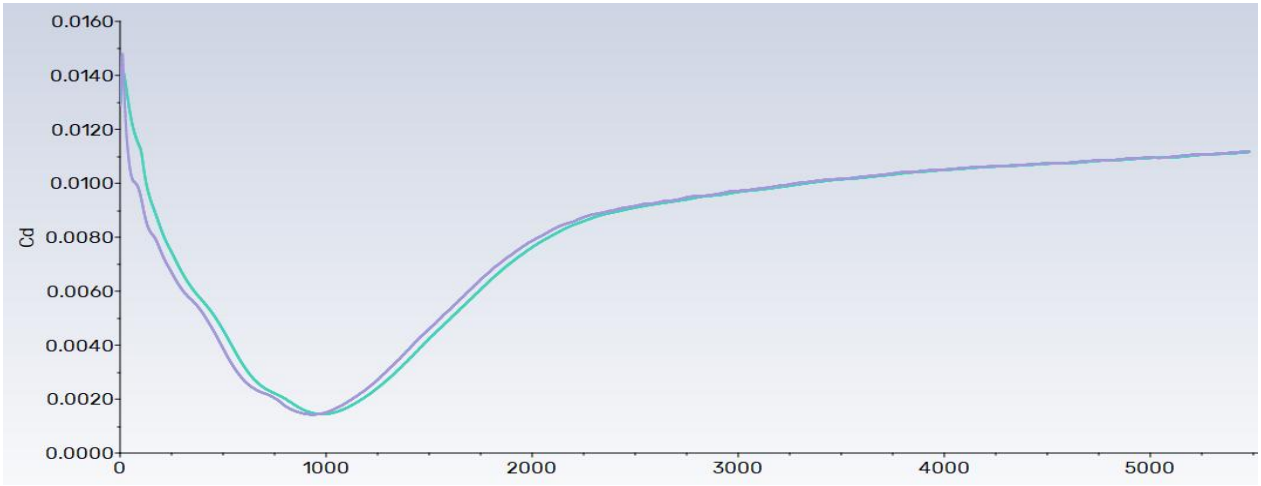

Figure 10 Cd with microjet at α =0

XI. CONCLUSION

The impact of jet-blowing direction on aerodynamic load management efficacy at subsonic and transonic speeds is investigated numerically in this work. The results show that while both upstream and conventional microjets can effectively reduce lift at a variety of angles of attack, the upstream jet is best at managing the load under the same circumstances. It makes sense since the upstream jet expands the flow separation zone compared to the conventional jet, which raises the suction surface pressure even more.

In terms of power consumption, the normal jets and the upstream jets are comparable in efficiency at low speeds. In transonic flows, the upstream jets not only reduce the lift but also mitigate the drag increase caused by the reinforced normal shock, resulting in a reduction of the overall power consumption.

Future research work is needed so that we can improve can contribute to the design of novel gust load alleviation systems in the future for more efficient and safer transport aircraft for reduced drag and emission.

REFERENCE

[1] F. M. Hoblit, "Gust Loads Fundamentals," in Gust Loads on Aircraft: Concepts and Applications, pp. 1–6, American Institute of Aeronautics and Astronautics, Washington, DC, USA, 1988.

[2] V. Handojo, Contribution to load alleviation in aircraft predesign and its influence on structural mass and fatigue, Technische Universitat, Berlin, Berlin, 2020, https://depositonce.tu-berlin.de/handle/11303/12111.

[3] T. E. Disney, "C-5a active load alleviation system," Journal of Spacecraft and Rockets, vol. 14, no. 2, pp. 81–86, 1977.

[4] J. F. Johnston, Accelerated development and flight evaluation of active controls concepts for subsonic transport aircraft. Volume 1: load alleviation/extended span development and flight tests, Technical Report NASA-CR-159097, NASA, 1979

[5] D. Heathcote, D. Cleaver, and I. Gursul, "Frequency response of aerodynamic load control through mini-tabs," in 55th AIAA Aerospace Sciences Meeting, American Institute of Aeronautics and Astronautics, 2017.

[6] J. P. Johnston and M. Nishi, "Vortex generator jets - means for flow separation control," AIAA Journal, vol. 28, no. 6, pp. 989– 994, 1990.

[7] R. H. Liebeck, "Design of subsonic airfoils for high lift," Journal of Aircraft, vol. 15, no. 9, pp. 547–561, 1978.

[8] R. Radespiel, M. Burnazzi, M. Casper, and P. Scholz, "Active flow control for high lift with steady blowing," Aeronautical Journal, vol. 120, no. 1223, pp. 171–200, 2016.

[9] S. Biringen, "Active control of transition by periodic suction blowing," Physics of Fluids, vol. 27, no. 6, p. 1345, 1984.

[10] K. Khalil, S. Asaro, and A. Bauknecht, "Active flow control devices for wing load alleviation," Journal of Aircraft, vol. 59, no. 2, pp. 458–473, 2022.

[11] M. G. Alexander, S. G. Anders, S. K. Johnson, J. P. Florance, and D. F. Keller, "Trailing edge blowing on a twodimensional six-percent thick elliptical circulation control airfoil up to transonic conditions," Technical Report NASA/TM2005-213545, NASA, 200

[12] Y. Li and N. Qin, "Airfoil gust load alleviation by circulation control," Aerospace Science and Technology, vol. 98, article 105622, 2020.

[13] N. H. Al-Battal, D. J. Cleaver, and I. Gursul, "Lift reduction by counter flowing wall jets," Aerospace Science and Technology, vol. 78, pp. 682–695, 2018.

[14] N. H. Al-Battal, D. J. Cleaver, and I. Gursul, "Unsteady actuation of counter-flowing wall jets for gust load attenuation," Aerospace Science and Technology, vol. 89, pp. 175–191, 2019.

[15] S. L. Krist, R. T. Biedron, and C. L. Rumsey, Cfl3d User's Manual (Version 5.0), The NASA Langley Research Center, Hampton, VA, 1998.

[16] B. Van Leer, "Upwind-difference methods for aerodynamic problems governed by the Euler equations," in Large-Scale Computations in Fluid Mechanics, Part 2, B. E. Engquist, S. Osher, and R. C. J. Somerville, Eds., pp. 327–336, American Mathematical Society, 1985.

[17] M. Blaylock, R. Chow, A. Cooperman, and C. P. van Dam, "Comparison of pneumatic jets and tabs for active aerodynamic load control," Wind Energy, vol. 17, pp. 1365–1384, 2013.

[18] A. Lefebvre, B. Dano, W. B. Bartow, M. Difronzo, and G. C. Zha, "Performance and energy

expenditure of coflow jet airfoil with variation of Mach number," Journal of Aircraft, vol. 53, no. 6, pp. 1757–1767, 2016.

[19] Eggert, C.A.a., CFD study of NACA 0018 airfoil with flow control. 2017: Hampton, Virginia: National Aeronautics and Space Administration, Langley Research Center, NASA/TM-2017-219602, 2017.

[20] de Vries, H., C. Boeije, I. Cleine, E. van Emden, G. Zwart, H. Stobbe, A. Hirschberg, and H. Hoeijmakers, Fluidic Load Control for Wind Turbine Blades. 47th AIAA Aerospace Sciences Meeting including The New Horizons Forum and Aerospace Exposition, AIAA 2009-684, 2009.